Specifications of 5G Cell Search

Subjects: Telecommunications | Computer Science, Hardware & Architecture
Contributor: Khalid Lodhi, Jayant Chhillar, Sumit J. Darak, Divisha Sharma

5G Cell Search (CS) is the first step for user equipment (UE) to initiate communication with the 5G node B (gNB) every time it is powered ON. In cellular networks, CS is accomplished via synchronization signals (SS) broadcasted by gNB. 5G 3rd generation partnership project (3GPP) specifications offer a detailed discussion on the SS generation at gNB, but a limited understanding of their blind search and detection is available.

Keywords: 3GPP ; 5G cell search ; 5G physical layer ; RFNoC

1. Introduction

In a cellular network, user equipment (UE) performs initial access (IA) to establish communication with the base station (BS) every time it is powered ON [1][2][3][4][5][6]. The IA comprises the downlink and uplink synchronizations. The downlink synchronization involves the cell search (CS), and acquisition of minimum system information (MSI) at the UE [2][7][8][9]. The first step, CS, allows the UE to obtain cell identity and synchronize with the BS in terms of symbol, slot, subframe, and frame timings [7][8][9]. After the CS, MSI acquisition provides information such as access type (barred, restricted, or unrestricted), carrier frequency and bandwidth, cell selection information (minimum receiver level), scheduling information, downlink/uplink configurations, etc. [2][10][11][12]. The uplink synchronization, via physical random access channel (PRACH), allows the base station to locate and instruct the UE to fine-tune the uplink timings such that uplink transmissions from multiple UEs are aligned in time irrespective of their distances from base-station [10][13][14]. In [15], CS is moved from UE to BS via code-book-based approach. However, this approach is not compatible with existing 3GPP standards.

5G 3rd generation partnership project (3GPP) specifications offer a detailed discussion on the SS generation at gNB, but limited understanding about their blind search and detection at UE is available [7][8][9][10][16][17][18]. Historically, it is left to be designed by equipment manufacturers.

The CS in 5G substantially evolved from 4G Long Term Evolution (LTE) [19][20][21][22][23]. The significant difference is the location of SS in the frequency domain. In 4G LTE, the SS is transmitted over the subcarriers in the middle of the carrier [19]. In 5G, the location is not fixed and is unknown, which means the UE needs to blindly search the SS over the entire carrier bandwidth [10]. To simplify the blind search, 3GPP introduced Global Synchronization Channel Number (GSCN) in 5G, which pre-defines possible positions where gNB can transmit SS. The SS bandwidth and overall transmission bandwidth in 5G are significantly wider; hence, SS detection requires multiple large-size correlators [4]. This makes the blind search computationally complex and time-consuming. Deep learning for CS may not be suitable for low latency applications [24]. Other blocks of the CS physical layer (PHY), including message generators, channel encoders, data modulators, scramblers, interleaves, and their counterparts in the receivers, are redesigned in 5G [25][26]. Thus, efficient design of 5G CS and in-depth performance analysis are essential to understand computational complexity and identify the limitations for future standard releases.

2. Specifications of 5G CS

2.1. 5G CS PHY

Researchers consider the n78 frequency band (3300–3800 MHz) in the frequency range 1, i.e., FR1 (410–7125 MHz) as it is being widely chosen for initial deployment of the 5G networks [5][6]. As per the 3GPP specifications, the maximum transmission bandwidth in the n78 band is 100 MHz, and sub-carriers (SC) spacing (SCS) is fixed to 30 kHz for SS [17]. Thus, the maximum number of SC in the n78 band is 3276. In 5G, a resource block (RB) is the smallest bandwidth unit for resource allocation and 1 RB consists of 12 SCs. Thus, the maximum number of RBs available in the n78 band is 273.

The 5G PHY is based on orthogonal frequency division multiplexing (OFDM) based waveform modulation [25]. Each OFDM symbol consists of the number of SCs which must be a power of two due to IFFT/FFT operations. This results in

4096 SCs per OFDM symbol in n78 [17]. In the time domain, each frame duration is 10 ms, and it consists of 10 sub-frames. Each sub-frame consists of 2 slots, and each slot consists of 14 OFDM symbols. Then, a single frame of 10 ms comprises 280 OFDM symbols. Then, the symbol duration is 33.33 µs with a cyclic prefix size of 2.86 µs for the first symbol of each slot and 2.34 µs for the remaining 13 symbols. Different size of cyclic prefix allows a common frame structure for multiple SCS newly introduced in 5G [5][25].

The SS signals are transmitted in a burst, known as SS burst (SSB), and the size, duration, and periodicity of the SSB depend on the operating frequency range. For n78, SSB is transmitted in every other frame, and each SSB comprises 8 SS [7][8][9][10][16][18]. In a frame, the starting OFDM symbol of the SS is {4,8,16,20,32,36,44,48}. The duration of each SS is 4 OFDM symbols which means SSB spans over 52 OFDM symbols in a frame of 280 symbols.

Each SS consists of 240 sub-carriers (SC) in the frequency domain, i.e., 20 resource blocks (RBs) and 4 OFDM symbols in the time domain [7][8][9][10][16][18]. As shown in **Figure 1**, the middle 127 SC of the first and third OFDM symbols are occupied by PSS and SSS, respectively. Since PSS and SSS are the first signals detected by UE during IA, they are carefully designed to enable blind detection with high reliability. 3GPP has adopted m-sequences to generate PSS $dPSS(n)$ and SSS $dSSS(n)$, $0 \le n < 127$ [16]. The rest of the 113 SCs of the first symbol are fixed to zero. The PSS and SSS allow the UE to detect the physical cell ID (PCI). In 5G, there are 3 candidate PSS sequences and 336 candidate SSS sequences which means the PCI range is from 0 to 1007 [16][18]. In the third symbol, there are 7 upper and 6 lower SC adjacent to the SSS fixed to zero, and the remaining SCs are occupied by a physical broadcast control channel (PBCH) carrying MIS and DMRS. The DMRS occupies 25% of the remaining SC, i.e., 144 SC. Since DMRS is quadrature phase shift keying (QPSK) demodulated, it consists of 288 bits which are generated using 3GPP defined pseudo-random sequence generator using two parameters: (1) PCI, $NCellID$, and (2) SS index, SSi, of the SS in SSB, $SSi\ i \in \{1,2,\ldots,8\}$ [16][18]. At UE, DMRS is detected after PSS and SSS detections which means DMRS allows estimation of the SS index which is critical for a frame, sub-frame, slot, and symbol synchronization. DMRS also allows channel estimation for MIS reception via PBCH [11][12][23].

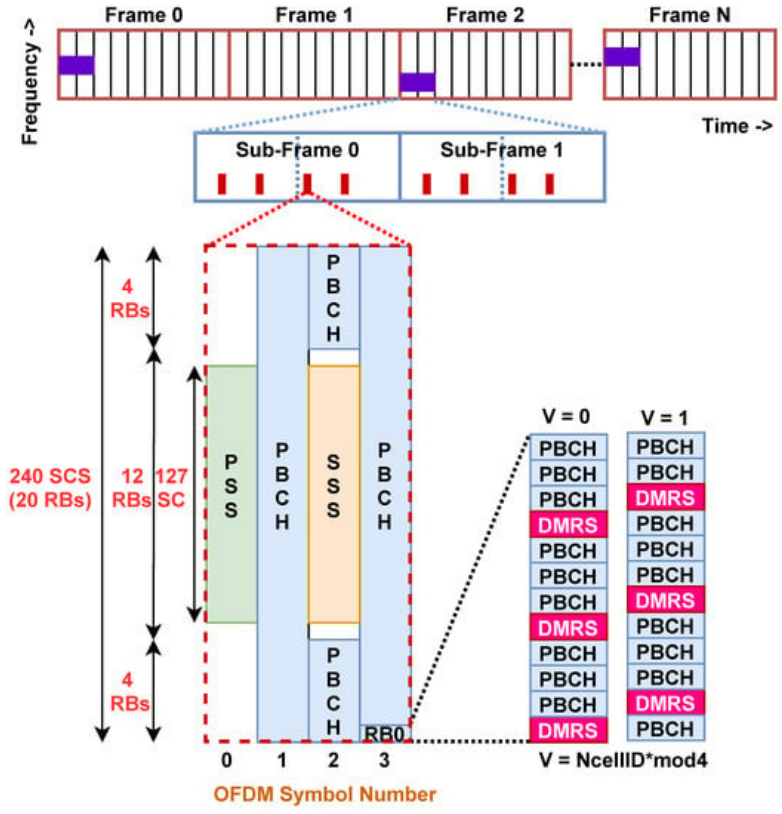

Figure 1. Details of 5G SSB scheduling and SS build blocks [16][18].

The location of all SS in SSB among 4096 SCs is not fixed in 5G and it is decided by the GSCN value. Furthermore, gNB can dynamically change the GSCN of the SSB. As per 3GPP specifications, there is a one-to-one mapping between the GSCN value and corresponding SSB center frequency [16][18]. In n78, the GSCN range is from 7711–8051 and the frequency resolution is 1.44 MHz. For example, the carrier frequency of 3305.28 Mhz is assigned a GSCN of 7711. Then, the GSCN of 7712 corresponds to the carrier frequency of 3305.28 + 1.44 = 3306.72 MHz. The last GSCN of the n78 band is 8051 and it corresponds to 3794.88 MHZ [16][18]. Such a GSCN raster of 1.44 MHz resolution allows UE to quickly detect SS by limiting the search over a limited number of center frequencies compared to the search over carrier frequencies with a channel raster of 15 kHz resolution.

2.2. Review: Mapping of 5G CS PHY on Hardware

The design, theoretical analysis, and simulation-based performance evaluation of 5G PHY have been an active research topic in the last few years [7][8][9][13][14][27][28]. Various works on the design and optimization of PHY sub-blocks such as channel encoders [29][30][31][32], OFDM modulator [33][34], beamforming [35][36] and channel estimation [37][38][39] have been explored to improve the PHY performance compared to 4G PHY. However, only a few works have focused on 3GPP standards and further improvements without compromising the compatibility with existing and previous standards [7][8][13][14][19][28]. From 5G CS perspectives, works in [8][9] provide an in-depth understanding of the SS generation while [7] offers an innovative intelligence-based CS approach. However, these works do not highlight the challenges in SS detection and applications of SS detection for timing synchronization.

Another important aspect of 5G PHY deployment is an efficient implementation on the software and hardware platforms. Compared to 4G, there are numerous scenarios that have resulted in the split of PHY depending on positions of radio, distribution, and centralized units [40][41][42]. This demands hardware-software co-design of the PHY. In [43][44], authors have explored the hardware-software co-design of IEEE 802.11 PHY on Zynq system-on-chip (SoC) platform. In [33][45], authors have explored reconfigurable OFDM waveform with dynamically controlled out-of-band emission. In [46], authors have proposed reconfigurable OFDM-based PHY to support multi-standard operations. However, none of these works consider 3GPP compatible 5G PHY. The work in [26] is limited to OFDM-based transceivers but does not consider various control and data channels in 5G while the work in [47] is limited to software-based CS implementation using USRP.

References

1. Won, S.; Choi, S.W. Three Decades of 3GPP Target Cell Search through 3G, 4G, and 5G. IEEE Access 2020, 8, 116914–116960.
2. Lien, S.Y.; Shieh, S.L.; Huang, Y.; Su, B.; Hsu, Y.L.; Wei, H.Y. 5G New Radio: Waveform, Frame Structure, Multiple Access, and Initial Access. IEEE Commun. Mag. 2017, 55, 64–71.
3. Dahlman, E.; Parkvall, S. NR—The New 5G Radio-Access Technology. In Proceedings of the 2018 IEEE 87th Vehicular Technology Conference (VTC Spring), Porto, Portugal, 3–6 June 2018; pp. 1–6.
4. Jeon, J. NR Wide Bandwidth Operations. IEEE Commun. Mag. 2018, 56, 42–46.
5. Zaidi, A.A.; Baldemair, R.; Moles-Cases, V.; He, N.; Werner, K.; Cedergren, A. OFDM Numerology Design for 5G New Radio to Support IoT, eMBB, and MBSFN. IEEE Commun. Stand. Mag. 2018, 2, 78–83.
6. Lin, X.; Li, J.; Baldemair, R.; Cheng, J.F.T.; Parkvall, S.; Larsson, D.C.; Koorapaty, H.; Frenne, M.; Falahati, S.; Grovlen, A.; et al. 5G New Radio: Unveiling the Essentials of the Next Generation Wireless Access Technology. IEEE Commun. Stand. Mag. 2019, 3, 30–37.
7. Won, S.; Choi, S.W. A Tutorial on 3GPP Initial Cell Search: Exploring a Potential for Intelligence Based Cell Search. IEEE Access 2021, 9, 100223–100263.
8. Chakrapani, A. On the Design Details of SS/PBCH, Signal Generation and PRACH in 5G-NR. IEEE Access 2020, 8, 136617–136637.
9. Omri, A.; Shaqfeh, M.; Ali, A.; Alnuweiri, H. Synchronization Procedure in 5G NR Systems. IEEE Access 2019, 7, 41286–41295.
10. Dahlman, E.; Parkvall, S.; Sköld, J. Chapter 16—Initial Access. In 5G NR: The Next Generation Wireless Access Technology; Dahlman, E., Parkvall, S., Sköld, J., Eds.; Academic Press: Cambridge, MA, USA, 2018; pp. 311–334.
11. Zhang, C.; Wu, Q.; Zhao, X.; Bai, J.; Wang, Z. A Scheme for improving 5G Cell Search Performance. In Proceedings of the 2023 5th International Conference on Communications, Information System and Computer Engineering (CISCE), Guangzhou, China, 14–16 April 2023; pp. 141–145.
12. Wang, S.D.; Wang, H.M.; Wang, W.; Leung, V.C.M. Detecting Intelligent Jamming on Physical Broadcast Channel in 5G NR. IEEE Commun. Lett. 2023, 27, 1292–1296.
13. Zhang, Z. Novel PRACH Scheme for 5G Networks Based on Analog Bloom Filter. In Proceedings of the 2018 IEEE Global Communications Conference (GLOBECOM), Abu Dhabi, United Arab Emirates, 9–13 December 2018; pp. 1–7.
14. Schreiber, G.; Tavares, M. 5G New Radio Physical Random Access Preamble Design. In Proceedings of the 2018 IEEE 5G World Forum (5GWF), Silicon Valley, CA, USA, 9–11 July 2018; pp. 215–220.
15. Yin, J.L.; Lee, M.C.; Hsiao, W.H.; Huang, C.C. A Novel Network Resolved and Mobile Assisted Cell Search Method for 5G Cellular Communication Systems. IEEE Access 2022, 10, 75331–75342.

16. 3GPP. NR: Physical Channels and Modulation; Technical Specification (TS) 36.211, Version 17.0; 3rd Generation Partnership Project (3GPP): Valbonne, France, 2022.
17. 3GPP. NR: Physical Layer: General Description; Technical Specification (TS) 36.201, Version 17.0.0; 3rd Generation Partnership Project (3GPP): Valbonne, France, 2022.
18. 3GPP. NR: Physical Layer Procedures for Control; Technical Specification (TS) 36.213, Version 17.2.0; 3rd Generation Partnership Project (3GPP): Valbonne, France, 2022.
19. Zhang, Z.; Liu, J.; Long, K. Low-Complexity Cell Search With Fast PSS Identification in LTE. IEEE Trans. Veh. Technol. 2012, 61, 1719–1729.
20. Dahlman, E.; Parkvall, S.; Sköld, J. Chapter 5—NR Overview. In 5G NR: The Next Generation Wireless Access Technology; Dahlman, E., Parkvall, S., Sköld, J., Eds.; Academic Press: Cambridge, MA, USA, 2018; pp. 57–71.
21. Dahlman, E.; Parkvall, S.; Sköld, J. Chapter 4—LTE—An Overview. In 5G NR: The Next Generation Wireless Access Technology; Dahlman, E., Parkvall, S., Sköld, J., Eds.; Academic Press: Cambridge, MA, USA, 2018; pp. 39–55.
22. Enescu, M.; Yuk, Y.; Vook, F.; Ranta-aho, K.; Kaikkonen, J.; Hakola, S.; Farag, E.; Grant, S.; Manolakos, A. PHY Layer. In 5G New Radio: A Beam-Based Air Interface; John Wiley & Sons: Hoboken, NJ, USA, 2020; pp. 95–260.
23. Chong, D.; Ko, G.; Kim, B.K.; Do, J.H.; Lee, J. Efficient PBCH DMRS Sequence Detection for Fast Synchronization Process of 5G NR Systems. In Proceedings of the 2021 IEEE 94th Vehicular Technology Conference (VTC2021-Fall), Norman, OK, USA, 27–30 September 2021; pp. 1–5.
24. Wang, M.; Hu, D.; He, L.; Wu, J. Deep-Learning-Based Initial Access Method for Millimeter-Wave MIMO Systems. IEEE Wirel. Commun. Lett. 2022, 11, 1067–1071.
25. Ahmadi, S. Chapter 3—New Radio Access Physical Layer Aspects (Part 1). In 5G NR; Ahmadi, S., Ed.; Academic Press: Cambridge, MA, USA, 2019; pp. 285–409.
26. Bishop, J.; Chareau, J.M.; Bonavitacola, F. Implementing 5G NR Features in FPGA. In Proceedings of the 2018 European Conference on Networks and Communications (EuCNC), Ljubljana, Slovenia, 18–21 June 2018; pp. 373–379.
27. Vook, F.W.; Ghosh, A.; Diarte, E.; Murphy, M. 5G New Radio: Overview and Performance. In Proceedings of the 2018 52nd Asilomar Conference on Signals, Systems, and Computers, Pacific Grove, CA, USA, 28–31 October 2018; pp. 1247–1251.
28. Lagen, S.; Wanuga, K.; Elkotby, H.; Goyal, S.; Patriciello, N.; Giupponi, L. New Radio Physical Layer Abstraction for System-Level Simulations of 5G Networks. In Proceedings of the ICC 2020–2020 IEEE International Conference on Communications (ICC), Dublin, Ireland, 7–11 June 2020; pp. 1–7.
29. Ji, W.; Wu, Z.; Zheng, K.; Zhao, L.; Liu, Y. Design and Implementation of a 5G NR System Based on LDPC in Open Source SDR. In Proceedings of the 2018 IEEE Globecom Workshops (GC Wkshps), Abu Dhabi, United Arab Emirates, 9–13 December 2018; pp. 1–6.
30. Henarejos, P.; Ángel Vázquez, M. Decoding 5G-NR Communications VIA Deep Learning. In Proceedings of the ICASSP 2020—2020 IEEE International Conference on Acoustics, Speech and Signal Processing (ICASSP), Barcelona, Spain, 4–8 May 2020; pp. 3782–3786.
31. Sybis, M.; Wesolowski, K.; Jayasinghe, K.; Venkatasubramanian, V.; Vukadinovic, V. Channel Coding for Ultra-Reliable Low-Latency Communication in 5G Systems. In Proceedings of the 2016 IEEE 84th Vehicular Technology Conference (VTC-Fall), Montreal, QC, Canada, 18–21 September 2016; pp. 1–5.
32. Gamage, H.; Rajatheva, N.; Latva-aho, M. Channel coding for enhanced mobile broadband communication in 5G systems. In Proceedings of the 2017 European Conference on Networks and Communications (EuCNC), Oulu, Finland, 12–15 June 2017; pp. 1–6.
33. Tewari, A.; Singh, N.; Darak, S.J.; Kizheppatt, V.; Jafri, M.S. Reconfigurable Wireless PHY with Dynamically Controlled Out-of-Band Emission on Zynq SoC. In Proceedings of the 65TH IEEE International Midwest Symposium on Circuits and Systems (MWSCAS 2022), Fukuoka, Japan, 7–10 August 2022; pp. 1–6.
34. Zhang, L.; Ijaz, A.; Xiao, P.; Molu, M.M.; Tafazolli, R. Filtered OFDM Systems, Algorithms, and Performance Analysis for 5G and Beyond. IEEE Trans. Commun. 2018, 66, 1205–1218.
35. Hong, W.; Choi, J.; Park, D.; Kim, M.s.; You, C.; Jung, D.; Park, J. mmWave 5G NR Cellular Handset Prototype Featuring Optically Invisible Beamforming Antenna-on-Display. IEEE Commun. Mag. 2020, 58, 54–60.
36. Herranz, C.; Zhang, M.; Mezzavilla, M.; Martin-Sacristán, D.; Rangan, S.; Monserrat, J.F. A 3GPP NR Compliant Beam Management Framework to Simulate End-to-End MmWave Networks. In Proceedings of the 21st ACM International

Conference on Modeling, Analysis and Simulation of Wireless and Mobile Systems, New York, NY, USA, 28 October–2 November 2018; pp. 119–125.

37. Mehrabi, M.; Mohammadkarimi, M.; Ardakani, M.; Jing, Y. Decision Directed Channel Estimation Based on Deep Neural Network k-Step Predictor for MIMO Communications in 5G. IEEE J. Sel. Areas Commun. 2019, 37, 2443–2456.
38. He, H.; Wen, C.K.; Jin, S.; Li, G.Y. Deep Learning-Based Channel Estimation for Beamspace mmWave Massive MIMO Systems. IEEE Wirel. Commun. Lett. 2018, 7, 852–855.
39. Chun, C.J.; Kang, J.M.; Kim, I.M. Deep Learning-Based Channel Estimation for Massive MIMO Systems. IEEE Wirel. Commun. Lett. 2019, 8, 1228–1231.
40. Larsen, L.M.P.; Checko, A.; Christiansen, H.L. A Survey of the Functional Splits Proposed for 5G Mobile Crosshaul Networks. IEEE Commun. Surv. Tutor. 2019, 21, 146–172.
41. Koutsopoulos, I. The Impact of Baseband Functional Splits on Resource Allocation in 5G Radio Access Networks. In Proceedings of the IEEE INFOCOM 2021—IEEE Conference on Computer Communications, Vancouver, BC, Canada, 10–13 May 2021; pp. 1–10.
42. Rony, R.I.; Lopez-Aguilera, E.; Garcia-Villegas, E. Optimization of 5G Fronthaul Based on Functional Splitting at PHY Layer. In Proceedings of the 2018 IEEE Global Communications Conference (GLOBECOM), Abu Dhabi, United Arab Emirates, 9–13 December 2018; pp. 1–7.
43. Drozdenko, B.; Zimmermann, M.; Dao, T.; Leeser, M.; Chowdhury, K. High-level hardware-software co-design of an 802.11a transceiver system using Zynq SoC. In Proceedings of the 2016 IEEE Conference on Computer Communications Workshops (INFOCOM WKSHPS), San Francisco, CA, USA, 10–14 April 2016; pp. 682–683.
44. Drozdenko, B.; Zimmermann, M.; Dao, T.; Chowdhury, K.; Leeser, M. Hardware-Software Codesign of Wireless Transceivers on Zynq Heterogeneous Systems. IEEE Trans. Emerg. Top. Comput. 2018, 6, 566–578.
45. Garg, S.; Agrawal, N.; Darak, S.J.; Sikka, P. Spectral coexistence of candidate waveforms and DME in air-to-ground communications: Analysis via hardware software co-design on Zynq SoC. In Proceedings of the 2017 IEEE/AIAA 36th Digital Avionics Systems Conference (DASC), St. Petersburg, FL, USA, 17–21 September 2017; pp. 1–6.
46. Pham, T.H.; Fahmy, S.A.; McLoughlin, I.V. An End-to-End Multi-Standard OFDM Transceiver Architecture Using FPGA Partial Reconfiguration. IEEE Access 2017, 5, 21002–21015.
47. Drozdova, V.G.; Kalachikov, A.A. SDR Based Evaluation of the Initial Cell Search In 5G NR OpenAirInterface Implementation. In Proceedings of the 2021 XV International Scientific-Technical Conference on Actual Problems of Electronic Instrument Engineering (APEIE), Novosibirsk, Russia, 19–21 November 2021; pp. 248–251.
